

in temperature as the jet pressure ratio increases to its maximum possible reliable limit ($P_{oj}/P_a = 2.1$). Beyond this limit it was hard to keep the supply pressure constant long enough to have reliable results. For jet stagnation pressures ($1.43 \leq P_{oj}/P_a \leq 2.1$), the following linear empirical equation was obtained:

$$T = 230 + 444 (P_{oj}/P_a - 1.43) C$$

At higher pressures, the cylindrical resonator is expected to yield higher temperatures, as suggested by this equation. This was not verified experimentally, due to the difficulties encountered in maintaining the jet pressure long enough to obtain a temperature reading.

Concluding Remarks

A new and improved axisymmetric resonator was introduced and tested. The results were compared with those obtained using the original model and the following conclusions were drawn:

1) Highly symmetrical implosions are possible to obtain, and depend not only on the symmetry of the device but on its four parameters studied here, namely, the disk diameter, nozzle width, and disk and plug positions. For a given nozzle diameter and width, there exists, for every disk diameter, an optimum position for both the disk and the plug. For the 89-mm nozzle diameter and the 5.1-mm nozzle width, the optimum plug and disk positions are given in Table 1.

2) Resonant oscillations can be obtained for a wide range of jet stagnation pressures and not restricted to a single value, as in the original model. The higher the jet pressure, the higher is the pressure amplitude, as shown in Fig. 4.

3) To minimize the effects of the boundary layers, the disk diameter to cylindrical cavity width ratio should be less than 10. Smaller nozzle and cavity widths were found to weaken the oscillations, which become almost nonexistent at higher pressures.

4) The steady-state temperatures were found to vary linearly with the jet stagnation pressures. For jet stagnation pressures ($1.43 \leq P_{oj} \leq 2.1$), a linear empirical equation was obtained. These values are about five times those measured with a logarithmic spiral resonance tube,⁵ thus making the proposed model a better ignitor over any of the existing ones. Future work should include the use of different gases, such as helium and hydrogen, which were previously found to yield temperatures about six times that obtained with air,⁶ as well as testing of the new model for its ability to ignite various gaseous mixtures.

Acknowledgment

The present work is supported by the Natural Sciences and Engineering Research Council of Canada under Grant A-4206.

References

- Wu, J. H. T., Ostrowski, P. P., Neemeh, R. A., and Lee, P., "Experimental Investigation of a Cylindrical Resonator," *AIAA Journal*, Vol. 12, Aug. 1974, pp. 1076-1078.
- Wu, J. H. T., Ostrowski, P. P., and Neemeh, R. A., "Cylindrical Shock Waves in a Resonator," *Proceedings of the 10th International Symposium on Shock Tubes and Waves*, Shock Tube Research Society, Kyoto, Japan, July 14-16, 1975, pp. 141-148.
- Sprenger, M., "Über Thermische Effekte in Resonanzrohren," *Mitt. Inst. Aerodynamik*, Zurich, Switzerland, No. 21, 1954, pp. 18-35.
- Neemeh, R. A., and Skarzynska, B., "Shock and Pressure Amplification in a Stepped Hartmann-Sprenger's Tube," *CAS Journal*, Vol. 34, No. 1, March 1988, pp. 48-54.
- Neemeh, R. A., Ostrowski, P. P., and Wu, J. H. T., "Thermal Performance of a Logarithmic-Spiral Resonance Tube," *AIAA Journal*, Vol. 22, Dec. 1984, pp. 1823-1825.
- Rakowsky, E. L., Corrado, A. A., and Marchesse, V. P., "Fluidic Explosive Initiator," Sixth Cranfield Fluidics Conf., BHRA Fluid Engineering, Cranfield, Bedford, England, UK, March 26-28, 1974, Paper H4, pp. 29-41.

Numerical Simulation of the Transient Ignition Regime of a Turbulent Diffusion Flame

D. Veynante,* F. Lacas,† and S. M. Candell‡
Ecole Centrale des Arts et Manufactures,
Chatenay-Malabry, France F92295

I. Introduction

MANY recent studies of turbulent combustion are based on flamelet models in which the reaction zone is treated as a collection of laminar flame elements (flamelets) embedded in the turbulent flow (Marble and Broadwell,¹ Peters,^{2,3} Bray⁴). An advantage of this concept is that it essentially decouples complex chemistry calculations from the turbulent flow description. Chemical kinetics and transport properties may be treated separately in a local flamelet analysis and then included in the calculation of the turbulent flowfield. Two different formulations of these flamelet models are generally available: one for turbulent premixed flames, the other for turbulent diffusion flames. However, in some situations, premixed and nonpremixed flame elements may co-exist in the same flow. This is the case, for example, in the stabilization of diffusion flames or during the ignition phase of a cryogenic rocket engine. In a first step, the cold reactants, fuel and oxidizer, mix to form a premixed fluid. Then, when ignition occurs due to some external process such as autoignition, by mixing with a hot gas stream or spark ignition, a premixed flame is formed. All premixed reactants are eventually consumed and a stabilized diffusion flame takes over. Combustion in a diesel engine also begins with the ignition of a premixed flame and ends with a diffusion flame. It appears that such a situation is not adequately described with classical flamelet models. A combined flamelet representation, based on the coherent flame model initially derived by Marble and Broadwell,¹ accounting for premixed and nonpremixed flame regimes is tested to describe the unsteady reactive flow configurations.

II. Combined Flamelet Model

The combined model devised in this article employs the basic assumptions of the coherent flame model of Marble and Broadwell. Details of this model may be found in Ref. 1, as well as in Veynante et al.,^{5,6} Lacas et al.,⁷ or Darabiha et al.⁸ The turbulent reactive flow is described as a collection of laminar flamelets which are convected and distorted by the turbulent motion but retain an identifiable structure. In this sense, the reaction sheets remain "coherent." The basic model combines the following elements: 1) a set of dynamic equations and closure rules describing the turbulent flow, 2) a local model for the laminar flame elements taking into account the effect of strain and providing the consumption rates per unit flame area, V_{D_i} , and 3) a balance equation for the flame area per unit volume Σ .

The mean consumption rates of the main species are then obtained from Σ and V_{D_i} according to:

$$\dot{W} = \rho V_{D_i} \Sigma \quad (1)$$

Received Aug. 7, 1989; revision received Jan. 2, 1990. Copyright © 1990 by the American Institute of Aeronautics and Astronautics, Inc. All rights reserved.

*Research Fellow, Laboratoire EM2C, CNRS. Member AIAA.

†Research Fellow, Laboratoire EM2C, CNRS.

‡Professor, Laboratoire EM2C, CNRS. Member AIAA.

The combined premixed/nonpremixed model retains and extends these general ideas. For the sake of clarity, it is presented in the simplest possible form. Consider a simple, one step, fast, and irreversible reaction $F + s O \rightarrow P$ where F is the fuel, O the oxidizer, s the mass stoichiometric ratio, and P the products. While the original coherent flame model uses a single flame surface density Σ , two quantities of this type are now introduced to represent the local area of diffusion flamelets (Σ^d) and the local area of premixed flamelets (Σ^p). In addition, it is also necessary to consider a third surface density Σ^c that represents a nonreactive mixing area separating the two nonpremixed reactants O and F . This area corresponds to disruptive holes in the flame sheet. The two reactants O and F may diffuse across these surface elements to form premixed gas as presented in Figs. 1a and 1b. Then, in a second step (Figs. 1c), this premixed fluid may be ignited to burn as a premixed flame. The consumption of this local premixed

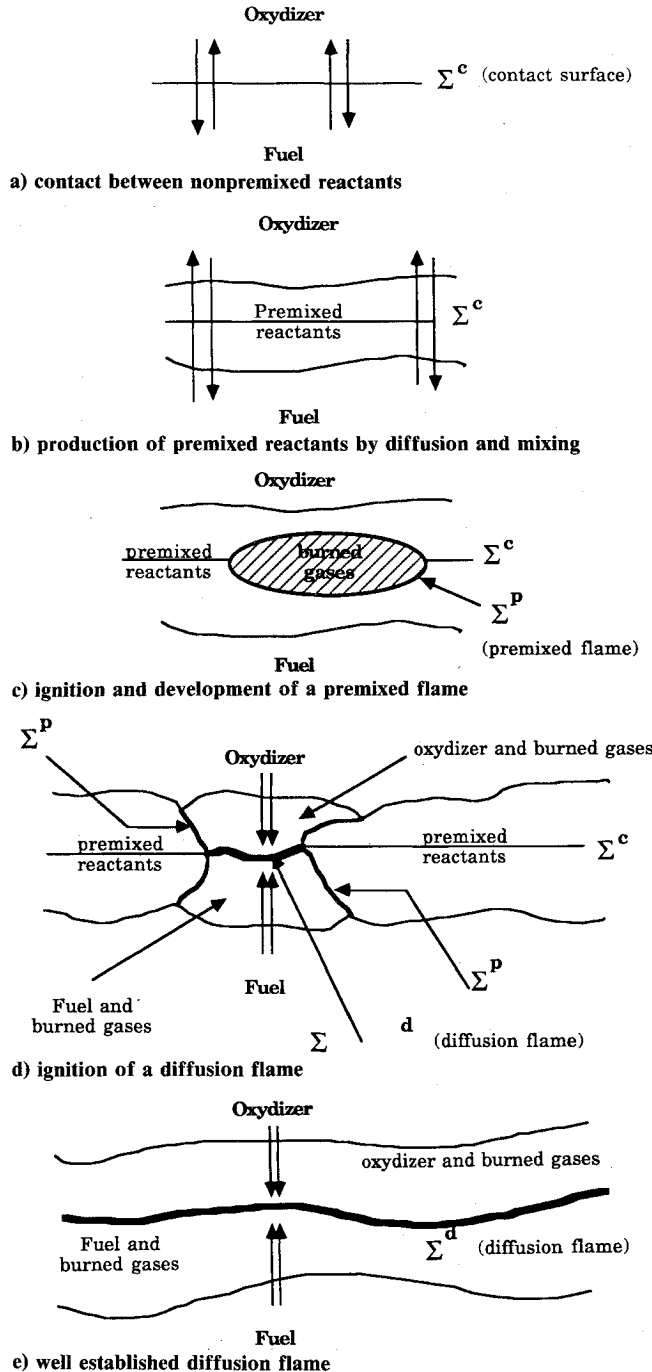


Fig. 1 Schematic representation of physical processes described in the combined premixed/nonpremixed flame model.

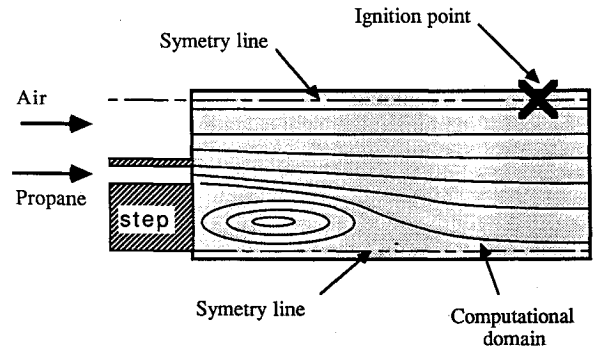


Fig. 2 Geometrical configuration used for numerical test.

stream eventually leads to a quenching of the premixed flame and serves as an initiation source to a diffusion flame involving the fuel and oxidizer (Fig. 1d). The last step of the process may be the consumption of all premixed reactants, leading to a state in which only a diffusion flame prevails between the unmixed oxidizer and fuel (Fig. 1e).

To be consistent with this description, it is necessary to introduce two mass fractions for each reactant i , one of which, Y_i^d , represents the mass of the reactant i in a nonpremixed form, whereas the other, Y_i^p , designates the mass of the reactant i premixed with the other reactant. From this analysis, the balance equation for the nonpremixed reactants may be written:

$$\frac{\partial \rho Y_i^d}{\partial t} + \frac{\partial \rho u_k Y_i^d}{\partial x_k} = \frac{\partial}{\partial x_k} \left(\frac{\mu_t}{\sigma_i^d} \frac{\partial \rho Y_i^d}{\partial x_k} \right) - \rho V_{D_i}^d \Sigma^d - \rho V_i^c \Sigma^c \quad (2)$$

where the last two terms express the consumption of reactant i in the diffusion flame sheets and the mixing of the two reactants O and F to form a premixed fluid. $V_{D_i}^d$ is the consumption rate per unit of diffusion flame area and V_i^c the mixing rate per unit of contact surface. For reactant i in premixed form, the balance equation becomes

$$\frac{\partial \rho Y_i^p}{\partial t} + \frac{\partial \rho u_k Y_i^p}{\partial x_k} = \frac{\partial}{\partial x_k} \left(\frac{\mu_t}{\sigma_i^p} \frac{\partial \rho Y_i^p}{\partial x_k} \right) - \rho V_{D_i}^p \Sigma^p + \rho V_i^c \Sigma^c \quad (3)$$

where the last two terms represent, respectively, the consumption rate of reactant i in a premixed flame and the production of premixed fluid through the mixing surface between nonpremixed reactants. Of course, the balance equation for the product P of the reaction is

$$\frac{\partial \rho Y_p}{\partial t} + \frac{\partial \rho u_k Y_p}{\partial x_k} = \frac{\partial}{\partial x_k} \left(\frac{\mu_t}{\sigma_p} \frac{\partial \rho Y_p}{\partial x_k} \right) + \rho V_{D_i}^d \Sigma^d + \rho V_p^p \Sigma^p \quad (4)$$

where the two source terms describe the generation of products in diffusion and premixed flamelets.

Now, three new equations are needed: one for each flame surface density considered. A balance equation for the diffusion flame surface density Σ^d may be written in the form

$$\begin{aligned} \frac{\partial \Sigma^d}{\partial t} + u_k \frac{\partial \Sigma^d}{\partial x_k} = & \frac{\partial}{\partial x_k} \left(\frac{V_t}{\sigma_\Sigma^d} \frac{\partial \Sigma^d}{\partial x_k} \right) + \alpha^d \epsilon_s \Sigma^d \\ & - \beta^d \left(\frac{V_{D_o}^d}{Y_o^d} + \frac{V_{D_f}^d}{Y_f^d} \right) (\Sigma^d)^2 + R^d \end{aligned} \quad (5)$$

where α^d and β^d are two constants and ϵ_s the local strain rate.

With the exception of its last term, this equation is similar to the balance equation proposed by Marble and Broadwell for the flame surface density in a diffusion flame. The last term, R^d , expresses the ignition of a diffusion flame by consumption of the premixed reactants between the nonpremixed reactants O and F (see Fig. 1d).

One may also write a balance equation for the premixed flame surface density, Σ^p :

$$\frac{\partial \Sigma^p}{\partial t} + u_k \frac{\partial \Sigma^p}{\partial x_k} = \frac{\partial}{\partial x_k} \left(\frac{V_t}{\sigma_k^d} \frac{\partial \Sigma^p}{\partial x_k} \right) + \alpha^p \epsilon_s \Sigma^p - \beta^p \left(\frac{V_{D_o}^p}{Y_o^p} + \frac{V_{D_f}^p}{Y_f^p} \right) (\Sigma^p)^2 + f_{\text{ign}} \quad (6)$$

where α^p and β^p are two new constants.

The production of a premixed flame surface due to the ignition of premixed reactants is expressed by the last term of this equation, f_{ign} . This function is determined from a local analysis of the flow conditions at the initial instant and it depends on the process utilized to ignite the reactive stream (spark, mixing with hot gases etc.). In general, f_{ign} will be a function of the local mass fractions of premixed reactants, temperature, strain rate, energy release in the spark, etc.

The balance equation for the third surface density Σ^c , corresponding to contact elements, has logically the same form as the two others equations:

$$\frac{\partial \Sigma^c}{\partial t} + u_k \frac{\partial \Sigma^c}{\partial x_k} = \frac{\partial}{\partial x_k} \left(\frac{V_t}{\sigma_k^c} \frac{\partial \Sigma^c}{\partial x_k} \right) + \alpha^c \epsilon_s \Sigma^c - \beta^c \left(\frac{V_{D_o}^c}{Y_o^d} + \frac{V_{D_f}^c}{Y_f^d} \right) (\Sigma^c)^2 + R^c \quad (7)$$

where α^c and β^c are two constants.

The third term describes the mutual annihilation of contact surfaces due to complete mixing of the nonpremixed reactants separating adjacent contact sheets. The last term R^c expresses the dissipation of the contact surface by ignition of a diffusion flame between the two nonpremixed reactants.

Now, we must express the two source terms, R^d and R^c . R^d is the production of the diffusion flame surface by consumption

of the premixed reactants flowing between streams of pure oxidizer and fuel, whereas R^c corresponds to the destruction of contact elements by ignition of a diffusion flame between the nonpremixed reactants. Then, logically,

$$R^d = -R^c \quad (8)$$

R^d expresses the production of a diffusion flame resulting from the destruction of a premixed flame surface. This process is associated with the consumption of the fresh premixed intervening reactants. The destruction of a premixed flame area has been already included in the balance equation for premixed flame area [Eq. (6)]. Accordingly, R^d may be viewed as a part of this destruction term

$$R^d = \gamma^d \left[\frac{V_{D_o}^p}{Y_o^p} + \frac{V_{D_f}^p}{Y_f^p} \right] (\Sigma^p)^2 \quad (9)$$

We now have written a set of equations that simultaneously model premixed and nonpremixed turbulent flames. This set may be used to predict the ignition of a diffusion flame in a mixing layer.

As usual, this set of equations must be supplemented with expressions for the local consumption rates of each reactant in the premixed and diffusion flame sheets and with a mixing rate per unit of contact area, $V_{D_i}^p$, $V_{D_i}^d$, $V_{D_i}^c$, respectively. In general, these consumption rates are obtained from the computations of plane laminar strained flames including complex chemistry features and multicomponent transport (Darabiha et al.⁸), or from analytical expressions derived under the assumption of an infinitely fast, irreversible chemical reaction (Marble and Broadwell¹). However, for a simple test case, like the one proposed next, all the local consumption rates may be assumed to be constant.

III. Numerical Simulation of the Transient Ignition Phase of a Turbulent Diffusion Flame

The balance equations of mass, momentum, energy, species, and surface densities are discretized and solved using a finite-volume technique (Dupoirieux and Scherrer⁹). The $k-\epsilon$ closure scheme is adopted. The local strain rate is determined from the turbulent kinetic energy and dissipation according to $\epsilon_s = C_s \epsilon/k$. The ignition function is here replaced by an initial distribution of the premixed flame area at the ignition point.

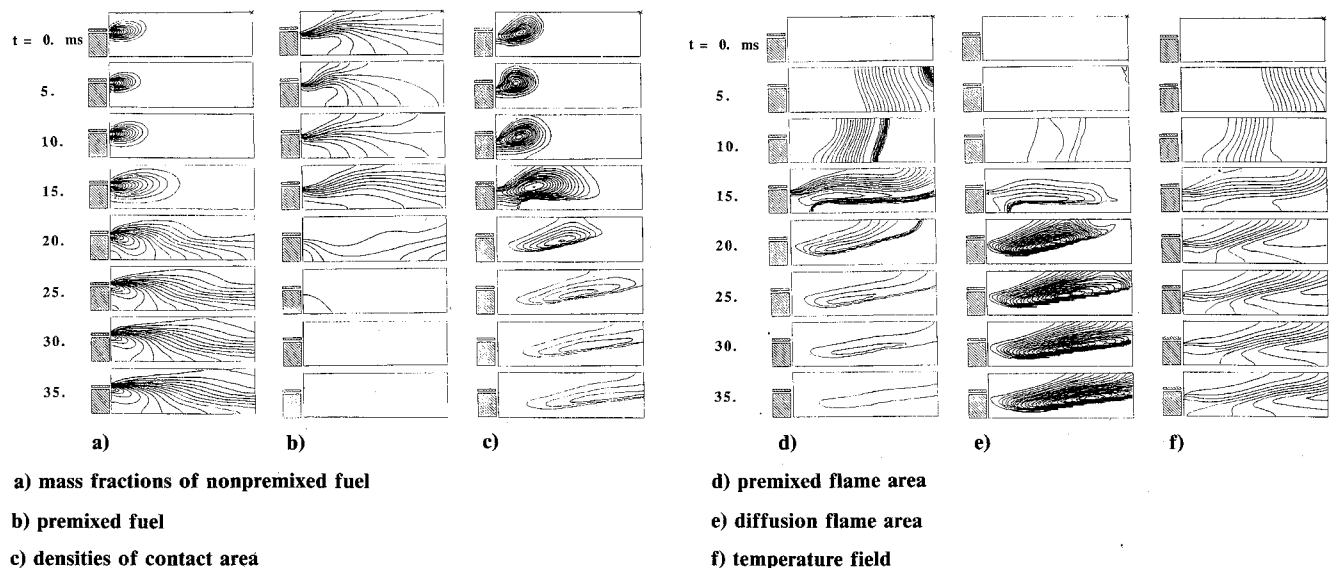


Fig. 3 Contours of constant various quantities as a function of time.

We now consider a numerical test of the model in the case of a two-dimensional mixing layer in the configuration shown in Fig. 2. Propane is injected through a narrow slot into a stream of air. In the first step, no combustion is taken into account. Only contact area is considered and the nonpremixed reactants mix to form a premixed stream. When the flow is well established, ignition takes place from the initial premixed flame area distributed at time $t = 0$ around the ignition point.

The contours of constant mass fractions of nonpremixed fuel, premixed fuel, densities of contact, premixed and diffusion flame areas and temperature are displayed in Fig. 3 as a function of time. Combustion begins with an unsteady premixed flame propagating in the initial mixture. The flame front travels crosswise and then propagates upstream inside the recirculation zone. A diffusion flame is then ignited and reaches a stationary configuration while the premixed flame disappears with the consumption of all the premixed reactants. This description is in qualitative agreement with a high-speed schlieren film of the ignition phase of an experimental combustor with the same geometrical configuration. The steady-state structure of the established diffusion flame is also in agreement with previous numerical simulations and experiments (Lacas et al.⁷).

IV. Conclusions

A model is proposed for turbulent flames combining premixed and nonpremixed flamelets. This model is tested in a simple case to simulate the transient post ignition regime of a diffusion flame. Further computations are being conducted to qualify the combined model. It will be useful to compare numerical predictions with experimental results, but the available data are not adequate. However, preliminary calculations indicate that it may be possible to describe time-evolving situations or the steady-state stabilization of nonpremixed shear flows. Further tests should prove whether this model is able to simulate blow-off and lift-off of diffusion flames. The formulation may be improved in various ways. For example, it will be easy to add other terms in the balance equations for the different flame surface densities to predict the quenching phenomenon due to excessively large local strain rates.

References

- ¹Marble, F. E., and Broadwell, J. E., "The Coherent Flame Model for Turbulent Chemical Reactions," TRW, EL Segundo, CA Project Squid Rept. TRW-9-PU, 1977.
- ²Peters, N., "Laminar Diffusion Flamelets in Nonpremixed Turbulent Combustion," *Progress in Energy and Combustion Science*, Vol. 10, No. 3, 1984 p. 319.
- ³Peters, N., "Laminar Flamelets Concepts in Turbulent Combustion," 21st Symposium (International) on Combustion, Combustion Inst., Pittsburgh, PA, 1986.
- ⁴Bray, K. N. C., "Methods of Including Realistic Chemical Mechanisms in Turbulent Combustion Models," *Second Workshop on Modeling of Chemical Reaction Systems*, Heidelberg, Germany, 1986.
- ⁵Veynante, D., Lacas, F., and Candel, S. M., "A New Flamelet Combustion Model Combining Premixed and Nonpremixed Turbulent Flames," AIAA Paper 89-0487, Jan. 1989.
- ⁶Veynante, D., Candel, S. M., and Martin, J. P., "Coherent Flame Modeling of Chemical Reactions in a Turbulent Mixing Layer," *2nd Workshop on Modeling of Chemical Reaction Systems*, Heidelberg, Germany, 1986.
- ⁷Lacas, F., Zikikout, S., and Candel, S. M., "A Comparison Between Calculated and Experimental Mean Source Terms in Nonpremixed Turbulent Combustion," AIAA Paper 87-1782, 1987.
- ⁸Darabiha, N., Giovangigli, V., Trouve, A., Candel, S. M. and Esposito, E., "Coherent Flame Description of Turbulent Premixed Ducted Flames," *Workshop on Turbulent Combustion*, Rouen, France, 1987.
- ⁹Dupouirieux, F., and Scherrer, D., "Méthodes Numériques à Convergence Rapide Utilisées pour le Calcul des Écoulements Réactifs," *1st Symposium on Numerical Simulation of Combustion Phenomena*, Sophia-Antipolis, France, May 1985.

Numerical Solutions of the Incompressible Navier-Stokes Equations with Boundary Condition Switching

Z. Fang* and I. Paraschivoiu†
École Polytechnique de Montréal,
Montréal, Québec, H3C 3A7 Canada

Introduction

THE boundary condition switching method for solving stream function-vorticity equations^{1,2} is applied to solve the incompressible Navier-Stokes equations in primitive variable form. The key idea of this method is that on boundaries, where both Dirichlet and Neumann boundary conditions are known, the Neumann boundary condition is satisfied naturally while the Dirichlet boundary condition is used to substitute the unknown boundary condition of the other variable, for instance, vorticity in stream function-vorticity equations and pressure in Navier-Stokes equations. When solving the Navier-Stokes equations with primitive variables for incompressible laminar flows, the Dirichlet boundary condition is the velocity boundary condition by giving zero velocity at wall boundaries. The Neumann boundary conditions are given by the continuity condition. In the methods solving Navier-Stokes equations with primitive variables, the velocity boundary conditions are implemented with the Neumann boundary condition satisfied by continuity equation. It is well known that these methods result in pressure oscillations using equal-order interpolation in finite element method³ (FEM) and using non-staggered grid in finite difference method⁴ (FDM). This difficulty could be removed by using the present method. Application of the present method is tested by both FEM and FDM. Our results show that this method does not result in any pressure oscillations. Thus, pressure solutions do not need to be filtered or smoothed.

Governing Equations and Boundary Conditions

The two-dimensional steady incompressible Navier-Stokes equations are

$$\mathbf{V} \cdot \nabla \mathbf{V} + \nabla P / \rho = \nu \nabla^2 \mathbf{V} \quad (1)$$

$$\nabla \cdot \mathbf{V} = 0 \quad (2)$$

in a bounded domain Ω , where \mathbf{V} is the velocity vector, P the pressure, ρ the density, and ν the kinematic viscosity. Boundary conditions are

$$\mathbf{V} = \mathbf{V}(x) \quad \text{on } \Gamma_1 \in \Gamma \equiv \partial\Omega \quad (3)$$

$$\frac{\partial \mathbf{V}}{\partial n} = \frac{\partial \mathbf{V}}{\partial n}(x) \quad \text{on } \Gamma_2 \in \Gamma \equiv \partial\Omega \quad (4)$$

$$P = P(x) \quad \text{on } \Gamma_3 \in \Gamma \equiv \partial\Omega \quad (5)$$

where $\Gamma_1 \cup \Gamma_2 \cup \Gamma_3 = \Gamma$.

On some boundaries both Dirichlet and Neumann boundary conditions for velocity exist when a viscous flow problem is

Received Dec. 21, 1989; revision received May 8, 1990; accepted for publication May 20, 1990. Copyright © 1990 by the American Institute of Aeronautics and Astronautics, Inc. All rights reserved.

*Research Associate, Department of Mechanical Engineering, P. O. Box 6079, Station A. Member AIAA.

†J.-A. Bombardier Aeronautical Chair Professor, Department of Mechanical Engineering, P. O. Box 6079, Station A. Member AIAA.